Numerical Heat Transfer, Part B: Fundamentals: An International Journal of Computation and Methodology

Publication details, including instructions for authors and subscription information:
http://www.tandfonline.com/loi/unhb20

Improvement of SIMPLER Algorithm for Incompressible Flow on Collocated Grid System

Y. P. Cheng [a], T. S. Lee [a], H. T. Low [a] & W. Q. Tao [b]

[a] Laboratory of Fluid Mechanics, Department of Mechanical Engineering, National University of Singapore, Singapore

[b] State Key Laboratory of Multiphase Flow in Power Engineering, School of Energy & Power Engineering, Xi'an Jiaotong University, Xi'an, Shaanxi, People's Republic of China

Available online: 14 May 2007

To cite this article: Y. P. Cheng, T. S. Lee, H. T. Low & W. Q. Tao (2007): Improvement of SIMPLER Algorithm for Incompressible Flow on Collocated Grid System, Numerical Heat Transfer, Part B: Fundamentals: An International Journal of Computation and Methodology, 51:5, 463-486

To link to this article: http://dx.doi.org/10.1080/10407790600939767

Numerical Heat Transfer, Part B, 51: 463–486, 2007

ISSN: 1040-7790 print/1521-0626 online
DOI: 10.1080/10407790600939767

Taylor & Francis
Taylor & Francis Group

IMPROVEMENT OF SIMPLER ALGORITHM FOR INCOMPRESSIBLE FLOW ON COLLOCATED GRID SYSTEM

Y. P. Cheng, T. S. Lee, and H. T. Low
Laboratory of Fluid Mechanics, Department of Mechanical Engineering, National University of Singapore, Singapore

W. Q. Tao
State Key Laboratory of Multiphase Flow in Power Engineering, School of Energy & Power Engineering, Xi'an Jiaotong University, Xi'an, Shaanxi, People's Republic of China

In this article an Improved SIMPLER (CLEARER) algorithm is proposed to solve incompressible fluid flow and heat transfer problems. Numerical study shows with the CLEARER algorithm on a collocated grid, in the correction stage the velocities on the main nodes are overcorrected with the pressure correction, which lowers the convergence rate; hence a second relaxation factor is introduced to overcome this disadvantage. By setting this factor less than the underrelaxation factor for velocities, the convergence performance can be significantly enhanced; meanwhile, the robustness can also be increased. Four numerical examples with reliable solutions are computed to validate the CLEARER algorithm, and the results show that this algorithm can predict the numerical results accurately. Compared with the SIMPLER algorithm, CLEARER can enhance the convergence rate greatly, and in some cases it only needs as little as 17% of the iterations required by SIMPLER to reach the same convergence criterion.

INTRODUCTION

Since the SIMPLE algorithm was first proposed by Patankar and Spalding [1], SIMPLE-like algorithms have been used extensively to solve incompressible fluid flow and heat transfer problems. Because a staggered grid has the advantage of preventing a checkerboard pressure field in the flow solution, the SIMPLE-like algorithms were implemented on staggered grids in the 1980s and before. On the staggered grid, the vector components and scalar variables are stored at different locations, being half a control-volume width apart in each coordinate, which will definitely increase the storage memory and computational time in the numerical simulation, especially in three-dimensional calculations. Furthermore, the staggered

Received 2 June 2006; accepted 12 June 2006.
The fourth author thanks for the support from the National Natural Science Foundation of China (50476046).
Address correspondence to T. S. Lee, Laboratory of Fluid Dynamics, Department of Mechanical Engineering, National University of Singapore, 10 Kent Ridge Crescent, 119260, Singapore. E-mail: mpeleets@nus.edu.sg

NOMENCLATURE

a	thermal diffusivity	β	relaxation factor, thermal expansion coefficient
a_P, a_E, a_W, a_N, a_S	coefficients in the discretized equation	γ	relaxation factor
A	surface area	Γ	nominal diffusion coefficient
b	source term	δ	gap width
C_p	specific heat	$\delta x, \delta y$	distance between two adjacent grid points in x and y directions
d_e, d_n	diffusion conductivity at the interface	$\Delta x, \Delta y$	distance between two adjacent interfaces in x and y directions
d_P	diffusion conductivity on the main node	η	dynamic viscosity
E	time-step multiple	θ	angle
f^+	parameter used for interpolation	ν	kinematic viscosity
Flow_{ch}	characteristic flow rate	ρ	fluid density
g	gravitational acceleration	ϕ	general variable
K_{eq}	equivalent conductivity	ω	annular velocity
L	length of cavity		
p	pressure		
p^*	temporary pressure	**Subscripts**	
p'	pressure correction	c	cool
R	radius	e, w, n, s	cell face
Ra	Rayleigh number	H	high
Re	Reynolds number	in	inner
$R_{\max}$	maximum relative mass flow rate unbalance of control volume	m	mean
		max	maximum
		nb	neighboring grid points
S_u, S_v, S_T, S_ϕ	source term	p	refers to pressure
T	temperature	P, E, W, N, S	grid points
u, v	velocity component in x and y directions	T	refers to temperature
		u, v	refers to u and v velocities
$\tilde{u}_e^0, \tilde{v}_n^0$	pseudo-velocity		
U, V	dimensionless velocity in x and y directions	**Superscripts**	
		u, v	coefficients related to u and v velocities
U_{Lid}	moving velocity of lid		
x, y	coordinates	0	resolution of the previous iteration
X, Y	dimensionless coordinates		
α	underrelaxation factor	*	intermediate value

arrangement also brings much difficulty to unstructured and curvilinear body-fitted grids. However, on a collocated grid all the vector variables and scalar variables are stored at the same location, which avoids the problems of staggered grids. In 1983, Rhie and Chow [2] proposed a momentum interpolation method to eliminate the checkerboard pressure. Subsequently, comparison between the staggered grid and collocated grid [3–5] showed that the SIMPLE-like algorithms on collocated grids can provide similarly accurate results and convergence rates as those on staggered grid. Therefore, the collocated grid is attracting more and more attention from researchers.

However, the use of the momentum interpolation method proposed by Rhie and Chow may cause additional problems. Majumdar [6] and Miller et al. [7] pointed out

independently that the solution using the original Rhie and Chow scheme is underrelaxation factor-dependent, although they can remove the false pressure field effectively. Then Majumdar [6] presented an iteration algorithm to overcome this dependency. Kobayashi and Pereira [8] also solved this problem by simply setting the underrelaxation factor equal to 1 before the momentum interpolation method is implemented, but this method may lower the robustness of the algorithm. Choi [9] found that the original Rhie and Chow method is also time-step size-dependent, and he proposed a new scheme to overcome this problem. However, by numerical example, Yu et al. [10] observed that the solutions from Choi's scheme are still time-step size-dependent, and they further reported that a checkerboard pressure field might be obtained for small underrelaxation factor and time-step size when Rhie and Chow's method is used. Later, Yu et al. [11] discussed the role of the interface velocity on the collocated grid, and recommended that all the interface velocities be obtained with the momentum interpolation method; then they proposed two momentum interpolation methods which are independent of both underrelaxation factor and time-step size.

In the SIMPLE-like pressure-correction algorithms, there are two stages at each iteration level, which are called the prediction stage and the correction stage. For each variable, the same underrelaxation factors are adopted in the two stages. Recently, Tao et al. [12, 13] proposed a novel segregated algorithm named CLEAR on the staggered grid, which was then extended to the collocated grid [14]. In the CLEAR algorithm, a second relaxation factor is introduced in the correction stage. Numerical experiments showed that iteration number can be reduced by a maximum of 85% compared to the SIMPLER algorithm. However, the robustness of the CLEAR algorithm may be a little less than that of SIMPLER algorithm.

Therefore, we can see that in order to make a reliable and efficient computation on a collocated grid, the following three aspects must be guaranteed: (1) the algorithm should avoid the checkerboard pressure field; (2) the convergent solution should be independent of the underrelaxation factor and time-step size; and (3) the algorithm should possess the required robustness. In order to develop a computation scheme on the collocated grid which possesses the above three features, in this article the SIMPLER algorithm on the collocated grid is first reviewed briefly. Then, by virtue of some successful practices, an Improved SIMPLER (CLEARER) algorithm is proposed. Four examples with benchmark solutions are provided to validate the new algorithm, and its performance is compared with that of the SIMPLER algorithm. Finally, some conclusions are drawn.

GENERAL REVIEW OF THE SIMPLER ALGORITHM

For simplicity, here we take two-dimensional steady incompressible laminar fluid in Cartesian coordinates as our example. The collocated grid system is shown in Figure 1. The governing equations are as follows.

Continuity equation:

$$\frac{\partial(\rho u_f)}{\partial x} + \frac{\partial(\rho v_f)}{\partial y} = 0 \tag{1}$$

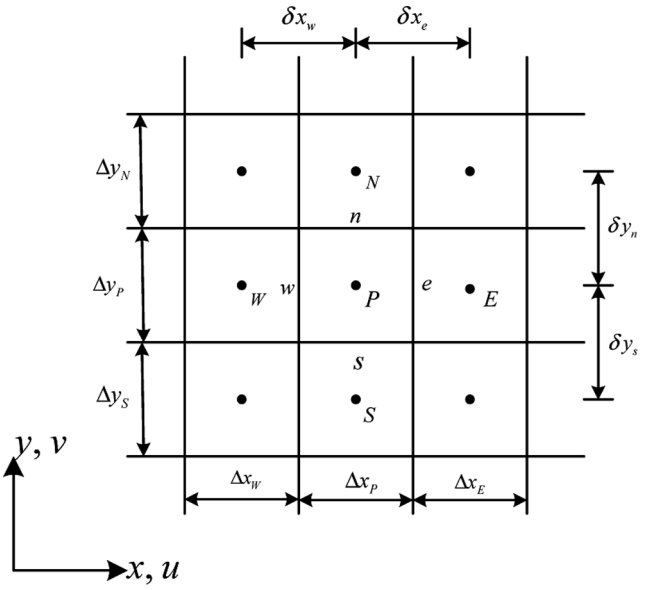

Figure 1. Control volumes of collocated grid in 2-D Cartesian coordinates.

Momentum equations:

$$\frac{\partial(\rho u_f u)}{\partial x} + \frac{\partial(\rho v_f u)}{\partial y} = -\frac{\partial p}{\partial x} + \eta\left(\frac{\partial^2 u}{\partial x^2} + \frac{\partial^2 u}{\partial y^2}\right) + S_u \tag{2a}$$

$$\frac{\partial(\rho u_f v)}{\partial x} + \frac{\partial(\rho v_f v)}{\partial y} = -\frac{\partial p}{\partial y} + \eta\left(\frac{\partial^2 v}{\partial x^2} + \frac{\partial^2 v}{\partial y^2}\right) + S_v \tag{2b}$$

Energy equation:

$$\frac{\partial(\rho u_f T)}{\partial x} + \frac{\partial(\rho v_f T)}{\partial y} = \frac{\lambda}{C_p}\left(\frac{\partial^2 T}{\partial x^2} + \frac{\partial^2 T}{\partial y^2}\right) + S_T \tag{3}$$

The above four equations can be recast in a general form:

$$\frac{\partial(\rho u_f \phi)}{\partial x} + \frac{\partial(\rho v_f \phi)}{\partial y} = \Gamma\left(\frac{\partial^2 \phi}{\partial x^2} + \frac{\partial^2 \phi}{\partial y^2}\right) + S_\phi \tag{4}$$

where u_f and v_f stand for the interface velocities whose interpolation scheme is the major issue on the collocated grid.

Equation (4) is discretized with the finite-volume method [15, 16] on the collocated grid and the source term S_ϕ is linearized as

$$S_\phi = S_C + S_P \phi_P \quad (S_P < 0) \tag{5}$$

By taking out the pressure gradient term from S_ϕ for the momentum equation, the final discretized equation can be written in this form with the underrelaxation factor incorporated.

$$\frac{a_P}{\alpha_u} u_P = a_E u_E + a_W u_W + a_N u_N + a_S u_S + b_P + \Delta y (p_w - p_e)_P + \frac{1-\alpha_u}{\alpha_u} a_P u_P^0 \tag{6a}$$

$$\frac{a_P}{\alpha_v} v_P = a_E v_E + a_W v_W + a_N v_N + a_S v_S + b_P + \Delta x (p_s - p_n)_P + \frac{1-\alpha_v}{\alpha_v} a_P v_P^0 \tag{6b}$$

where

$$b_P = S_C \, \Delta x \, \Delta y \tag{7}$$

The terms $(p_w)_P, (p_e)_P, (p_s)_P$, and $(p_n)_P$ are linearly interpolated from the neighboring nodes:

$$(p_w)_P = f_w^+ p_P + (1 - f_w^+) p_W \tag{8a}$$

$$(p_e)_P = f_e^+ p_E + (1 - f_e^+) p_P \tag{8b}$$

$$(p_s)_P = f_s^+ p_P + (1 - f_s^+) p_S \tag{8c}$$

$$(p_n)_P = f_n^+ p_N + (1 - f_n^+) p_P \tag{8d}$$

where

$$f_w^+ = \frac{\Delta x_W}{2\delta x_w} \qquad f_e^+ = \frac{\Delta x_P}{2\delta x_e} \qquad f_s^+ = \frac{\Delta y_S}{2\delta y_s} \qquad f_n^+ = \frac{\Delta y_P}{2\delta y_n} \tag{9}$$

In order to remove the influence of the underrelaxation factor, the modified momentum interpolation method (MMIM) proposed by Majumdar [6] is adopted here.

$$\begin{aligned} u_e &= \alpha_u \left(\frac{\sum a_{\mathrm{nb}} u_{\mathrm{nb}}^0 + b_P}{a_P} \right)_e + (1 - \alpha_u) u_e^0 + \frac{\alpha_u \Delta y (p_P - p_E)}{(a_P)_e} \\ &= \widetilde{u_e^0} + d_e (p_P - p_E) \end{aligned} \tag{10}$$

When the iteration converges, u_e and u_e^0 approach the same value, and this equation is equivalent to

$$u_e = \left(\frac{\sum a_{\mathrm{nb}} u_{\mathrm{nb}}^0 + b_P}{a_P}\right)_e + \frac{\Delta y(p_P - p_E)}{(a_P)_e} \tag{11}$$

which is independent of the underrelaxation factor α_u. Here

$$\begin{aligned}\widetilde{u_e^0} &= \alpha_u\left(\frac{\sum a_{\mathrm{nb}} u_{\mathrm{nb}}^0 + b_P}{a_P}\right)_e + (1-\alpha_u)u_e^0 \\ &= \alpha_u\left[f_e^+\left(\frac{\sum a_{\mathrm{nb}} u_{\mathrm{nb}}^0 + b_P}{a_P}\right)_E + (1-f_e^+)\left(\frac{\sum a_{\mathrm{nb}} u_{\mathrm{nb}}^0 + b_P}{a_P}\right)_P\right] \\ &\quad + (1-\alpha_u)u_e^0\end{aligned} \tag{12}$$

$$d_e = \frac{\alpha_u \Delta y}{(a_P)_e} = \frac{\alpha_u \Delta y}{f_e^+(a_P)_E + (1-f_e^+)(a_P)_P} \tag{13}$$

Similarly, the discretized momentum equation for the v component can be rewritten as

$$\begin{aligned}v_n &= \alpha_v\left(\frac{\sum a_{\mathrm{nb}} v_{\mathrm{nb}}^0 + b_P}{a_P}\right)_n + (1-\alpha_v)v_n^0 + \frac{\alpha_v \delta x(p_P - p_N)}{(a_P)_n} \\ &= \widetilde{v_n^0} + d_n(p_P - p_N)\end{aligned} \tag{14}$$

where

$$\begin{aligned}\widetilde{v_n^0} &= \alpha_v\left(\frac{\sum a_{\mathrm{nb}} v_{\mathrm{nb}}^0 + b_P}{a_P}\right)_n + (1-\alpha_v)v_n^0 \\ &= \alpha_v\left[f_n^+\left(\frac{\sum a_{\mathrm{nb}} v_{\mathrm{nb}}^0 + b_P}{a_P}\right)_N + (1-f_n^+)\left(\frac{\sum a_{\mathrm{nb}} v_{\mathrm{nb}}^0 + b_P}{a_P}\right)_P\right] \\ &\quad + (1-\alpha_v)v_n^0\end{aligned} \tag{15}$$

$$d_n = \frac{\alpha_v \Delta x}{(a_P)_n} = \frac{\alpha_v \Delta x}{f_n^+(a_P)_N + (1-f_n^+)(a_P)_P} \tag{16}$$

Substituting Eqs. (10) and (14) into the discretized continuity equation,

$$(\rho u)_e A_e - (\rho u)_w A_w + (\rho v)_n A_n - (\rho v)_s A_s = 0 \tag{17}$$

we have the following equation for pressure:

$$a_P p_P^* = \sum a_{\mathrm{nb}} p_{\mathrm{nb}}^* + b \tag{18}$$

where

$$a_P = a_E + a_W + a_N + a_S \tag{19}$$

$$a_E = (\rho Ad)_e \qquad a_W = (\rho Ad)_w \qquad a_N = (\rho Ad)_n \qquad a_S = (\rho Ad)_s \tag{20}$$

$$b = (\rho \widetilde{u^0} A)_w - (\rho \widetilde{u^0} A)_e + (\rho \widetilde{v^0} A)_s - (\rho \widetilde{v^0} A)_n \tag{21}$$

In the actual calculation, in order to increase the robustness of the algorithm, the pressure is also underrelaxed; then the final pressure equation can be recast with the underrelaxation factor incorporated:

$$\frac{a_P}{\alpha_P} p_P^* = \sum a_{\mathrm{nb}} p_{\mathrm{nb}}^* + b + \frac{1-\alpha_P}{\alpha_P} a_P p_P^0 \tag{22}$$

In order to let the intermediate velocities satisfy the continuity equation, the pressure corrections are added to them; the interface velocity correction terms are

$$u_e' = d_e(p_P' - p_E') \tag{23a}$$

$$v_n' = d_n(p_P' - p_N') \tag{23b}$$

The improved interface velocities can be expressed as

$$u_e = u_e^* + u_e' = u_e^* + d_e(p_P' - p_E') \tag{24a}$$

$$v_n = v_n^* + v_n' = v_n^* + d_n(p_P' - p_N') \tag{24b}$$

Substituting Eq. (24) into the discretized continuity Eq. (17),

$$a_P p_P' = \sum a_{\mathrm{nb}} p_{\mathrm{nb}}' + b \tag{25}$$

Here the coefficients $(a_P, a_E, a_W, a_N, a_S)$ are the same with those in the pressure Eq. (18); the only difference lies in the source term b, which can be calculated as follows:

$$b = (\rho u^* A)_w - (\rho u^* A)_e + (\rho v^* A)_s - (\rho v^* A)_n \tag{26}$$

Similarly, the velocities on the main nodes can also be corrected as follows:

$$u_P = u_P^* + d_P^u (p_w' - p_e')_P \tag{27a}$$

$$v_P = v_P^* + d_P^v (p_s' - p_n')_P \tag{27b}$$

where

$$d_P^u = \frac{\alpha_u \Delta y}{(a_P)_P} \qquad d_P^v = \frac{\alpha_v \Delta x}{(a_P)_P} \tag{28}$$

The pressure correction at the interface is linearly interpolated as

$$(p'_w)_P = f_w^+ p'_P + (1 - f_w^+) p'_W \tag{29a}$$

$$(p'_e)_P = f_e^+ p'_E + (1 - f_e^+) p'_P \tag{29b}$$

$$(p'_s)_P = f_s^+ p'_P + (1 - f_s^+) p'_S \tag{29c}$$

$$(p'_n)_P = f_n^+ p'_N + (1 - f_n^+) p'_P \tag{29d}$$

The computational steps of the CLEARER algorithm on the collocated grid can be summarized as follows.

Step 1. Assume the initial velocity field on the main nodes u_P^0 v_P^0 and at interfaces u_e^0 v_n^0.
Step 2. Calculate the discretized coefficients $(a_P, a_E, a_W, a_N, a_S)$ of the momentum equations, the discretized coefficients d_e[Eq. (13)] and d_n [Eq. (16)] for the pressure equation, and also the pseudo-velocities $\tilde{u}_e^0$ [Eq. (12)] and $\tilde{v}_n^0$ [Eq. (15)] to determine the source term [Eq. (21)] for the pressure equation based on the previous main node and interface velocities.
Step 3. Solve the discretized pressure equation [Eq. (22)] and obtain the pressure field p^*.
Step 4. Solve the discretized forms of the momentum equations [Eq. (6)] based on p^* to obtain the intermediate velocity field u_P^* and v_P^*.
Step 5. Calculate the interface velocities u_e^* and v_n^* with the MMIM based on u_P^*, v_P^*, and p^* to determine the source term [Eq. (26)] of the pressure-correction equation.
Step 6. Solve the pressure-correction equation [Eq. (25)], obtaining the pressure-correction value p'.
Step 7. Correct the interface velocities u_e and v_n with Eq. (24) and the velocities on the main nodes u_P v_P with Eq. (27).
Step 8. Solve the discretized equations of other scalar variables if necessary.
Step 9. Return to step 2 and repeat the process until the convergent solution is obtained.

From the procedure above, we can see that with the introduction of MMIM, the checkerboard pressure field can be damped out, and the solution is underrelaxation factor-independent.

MATHEMATICAL FORMULATION OF CLEARER

Discussion of the SIMPLER Algorithm

In the conventional SIMPLER algorithm stated above, in the corrector step after the pressure-correction equation is solved, both the main node velocities and interface velocities are improved with the pressure correction as shown in Eqs. (24) and (27). Our numerical experiment shows that it is appropriate to correct the interface velocities with the pressure correction; however, the velocities at the main nodes are overcorrected, hence the pressure correction should be underrelaxed

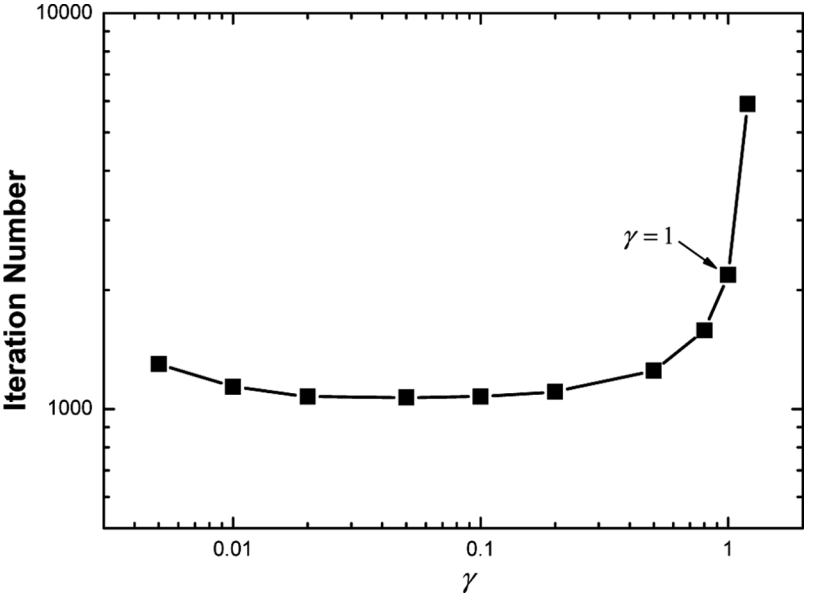

Figure 2. Influence of γ on the iteration number at $\alpha = 0.8$.

before it is used to correct the velocities at the main nodes.

$$u_P = u_P^* + \gamma_u d_P^u (p'_w - p'_e)_P \tag{30a}$$

$$v_P = v_P^* + \gamma_v d_P^v (p'_s - p'_n)_P \tag{30b}$$

For convenience, we set $\gamma_u = \gamma_v = \gamma$ and $\alpha_u = \alpha_v = \alpha$ hereafter.

Take the lid-driven flow in a square cavity as an example. Figure 2 shows the influence of the parameter γ on the iteration number when the underrelaxation factor for velocities $\alpha = 0.8$. In the conventional SIMPLER algorithm, $\gamma = 1$. When $\gamma > 1$, the iteration number will increase sharply, which shows that the pressure correction cannot be overrelaxed when the velocities at the main nodes are corrected. However, as γ is decreasing, the iteration number can be reduced greatly, even to 50% less than that at $\gamma = 1$. But if γ is decreasing further, the iteration number will increase mildly, but still stay less than that at $\gamma = 1$. Although the iteration number can be reduced by decreasing the value of γ, the solution will become oscillatory during the convergence progress, which will lower the robustness of the SIMPLER algorithm. Hence a new expression should be formulated to overcome this shortcoming while increasing the convergence rate.

Improved CLEARER Algorithm

In the SIMPLER algorithm, in both the predictor step and the corrector step, the same underrelaxation factor for each velocity component is adopted. Recently, a novel algorithm called CLEAR was proposed, in which the pressure equation

instead of the pressure-correction equation is used in the corrector step. Furthermore, in the corrector step, a second relaxation factor is introduced in determining the updated pseudo-velocity. Numerical examples show that with this method the convergence rate can be greatly speeded up compared with the SIMPLER algorithm. However, the robustness of the CLEAR algorithm is a little less than that of SIMPLER. Here we combine the advantages of the SIMPLER and CLEAR algorithms to formulate a new algorithm called CLEARER.

In the predictor step, CLEARER is the same as the SIMPLER and CLEAR algorithms; the only difference lies in the calculation of the interface velocities in the corrector step. As suggested by Yu et al. [11], the interface velocities in the correction stage are obtained with the momentum interpolation method; the details are as follows.

$$\begin{aligned} u_e^* &= \beta_u \left[\frac{\sum a_{\mathrm{nb}} u_{\mathrm{nb}}^* + b_P + \Delta y (p_P^* - p_E^*)}{a_P} \right]_e + (1-\beta_u) u_e^0 \\ &= \beta_u \left\{ f_e^+ \left[\frac{\sum a_{\mathrm{nb}} u_{\mathrm{nb}}^* + b_P + \Delta y (p_P^* - p_E^*)}{a_P} \right]_E \right. \\ &\quad \left. + (1-f_e^+) \left[\frac{\sum a_{\mathrm{nb}} u_{\mathrm{nb}}^* + b_P + \Delta y (p_P^* - p_E^*)}{a_P} \right]_P \right\} + (1-\beta_u) u_e^0 \end{aligned} \tag{31a}$$

$$\begin{aligned} v_n^* &= \beta_v \left[\frac{\sum a_{\mathrm{nb}} v_{\mathrm{nb}}^* + b_P + \Delta x (p_P^* - p_N^*)}{a_P} \right]_n + (1-\beta_v) v_n^0 \\ &= \beta_v \left\{ f_n^+ \left[\frac{\sum a_{\mathrm{nb}} v_{\mathrm{nb}}^* + b_P + \Delta x (p_P^* - p_N^*)}{a_P} \right]_N \right. \\ &\quad \left. + (1-f_n^+) \left[\frac{\sum a_{\mathrm{nb}} v_{\mathrm{nb}}^* + b_P + \Delta x (p_P^* - p_N^*)}{a_P} \right]_P \right\} + (1-\beta_v) v_n^0 \end{aligned} \tag{31b}$$

Here parameters β_u and β_v are the relaxation factors in calculating the interface velocities. When the iteration converges, u_e^* and v_n^* will approach u_e^0 and v_n^0, respectively, hence they are both independent of β_u and β_v. For convenience, we set $\beta_u = \beta_v = \beta$ hereafter. Then the improved interface velocities can be expressed as

$$u_e = u_e^* + d_e^* (p'_P - p'_E) \tag{32a}$$

$$v_n = v_n^* + d_n^* (p'_P - p'_N) \tag{32b}$$

Here

$$d_e^* = \frac{\Delta y}{(a_P)_e} \qquad d_n^* = \frac{\Delta x}{(a_P)_n} \tag{33}$$

The velocities at the main nodes can be updated as

$$u_P = u_P^* + d_P^{u*} (p'_w - p'_e)_P \tag{34a}$$

$$v_P = v_P^* + d_P^{v*} (p'_s - p'_n)_P \tag{34b}$$

where

$$d_P^{u*} = \frac{\Delta y}{(a_P)_P} \qquad d_P^{v*} = \frac{\Delta x}{(a_P)_P} \tag{35}$$

Substituting Eq. (32) into the continuity equation, the pressure-correction equation will be obtained. The solution procedure of this algorithm is almost the same as that of the SIMPLER algorithm, except that in step 5 the intermediate interface velocities are calculated according to Eq. (31), and in step 7 the velocities at the interfaces and main nodes are improved according to Eqs. (32) and (34). Hence, at every iterative level, the computational effort of CLEARER is identical with that of the SIMPLER algorithm.

Discussion of the Relaxation Factor β

In the SIMPLE-like segregated algorithms, the momentum equations and continuity equation are solved sequentially. In order to speed up the convergence rate, the momentum and continuity equations should be satisfied well at every iterative level, which is the aim of current SIMPLE variants. In the CLEARER algorithm, there are two parts to calculating the interface velocities as shown in Eq. (31): one is obtained from the momentum equation, and the other is the interface velocities at the previous iterative level which satisfy the continuity equation. By introducing the relaxation factor β, the relative weights of the two parts can be adjusted to make them match, so the convergence performance can be improved. It is notable that in Eqs. (33) and (35) the relaxation factor β can be incorporated, which will not influence the improved velocities because the pressure-correction equation is singular. In some cases β can be greater than 1, and when $\beta = \alpha$, CLEARER will become the SIMPLER algorithm. By reducing the value of β, the underrelaxation factor α can take larger value, which will increase the robustness of algorithm.

Figure 3 shows the influence of β on the iteration number at $\alpha = 0.8$ in lid-driven cavity flow. From this we can see that for the SIMPLER algorithm at $\beta = 0.8$, the convergence performance is not optimum. By decreasing the value of β, the iteration number can be greatly reduced, and it is only one-third at $\beta = 0.3$ of that at $\beta = 0.8$. Hence better convergence performance can be obtained by adjusting β than γ. However, similar to the influence of γ, with deceasing β, the required iteration number will be increased mildly. If the value of β is greater than α, the iteration number will also be increased greatly. Anyway, better convergence characteristics can be achieved by adjusting the value of β in a wide range below α. A similar phenomenon can also be found in other computational cases. The optimum value of β can be obtained by trial and error. In the following section the comparison of convergence performance is carried out under the optimum β.

VALIDATION OF CLEARER WITH NUMERICAL EXAMPLES

In order to verify the feasibility of the CLEARER algorithm on the collocated grid, four typical numerical examples with available solutions are computed: (1) lid-driven flow in a square cavity; (2) natural convection in a square cavity; (3) lid-driven

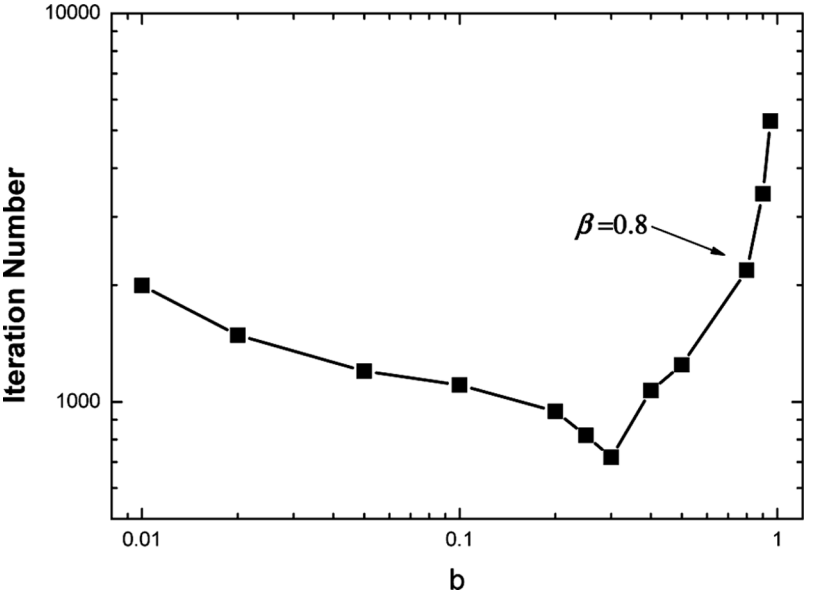

Figure 3. Influence of β on the iteration number at $\alpha = 0.8$.

flow in a polar cavity: and (4) natural convection in an annular enclosure. To make the comparison between CLEARER and SIMPLER meaningful, the numerical treatments of all other aspects should be kept the same. In both algorithms the stability-guaranteed second-order difference scheme (SGSD) [17] is adopted; the algebraic equations are solved by the alternating direction implicit method (ADI) [18] incorporating the block-correction technique [19]. For convenience, the time-step multiple E is adopted in the following presentation, which is related to the underrelaxation factor α by

$$E = \frac{\alpha}{1-\alpha} \qquad (0 < \alpha < 1) \tag{36}$$

The correspondence between α and E is presented in Table 1, which shows that with the time-step multiple, the performance of the algorithm in the high-value region of underrelaxation factor can be shown well.

The same convergence criterion is also used for two algorithms, as indicated below:

$$R_{\max} = \mathrm{MAX}\left[\frac{(\rho u^* A)_w - (\rho u^* A)_e + (\rho v^* A)_s - (\rho v^* A)_n}{\mathrm{Flow_{ch}}}\right] < 1.0 \times 10^{-8} \tag{37}$$

Table 1. Some correspondence between α and E

α	0.1	0.2	0.4	0.6	0.8	0.9	0.95	0.98	0.99
E	0.11	0.25	0.67	1.5	4	9	19	49	99

where $R_{\max}$ is the maximum relative mass flow rate imbalance of all the control volumes in the computational domain; Flow_{ch} is the characteristic flow rate through the centerline of the cavity; u^* and v^* are the intermediate interface velocities.

The same grid system for the two algorithms is used for the same problems. A uniform 51×51 grid is adopted for the first three cases, while for the last case the uniform grid 51×31 is used. The underrelaxation factor for pressure $\alpha_p = 0.9$, and for the natural-convection problem the underrelaxation factor for temperature $\alpha_T = 0.8$.

In the following four cases the computation conditions are introduced briefly, then numerical results with CLEARER are compared with the benchmark solution to test its accuracy, followed by comparison of the iteration number between the two algorithms with the variation of underrelaxation factor α. Furthermore, the ratio of the iteration number between CLEARER and SIMPLER algorithms with α is also provided. Because there is the same computational effort at every iterative level, the ratio of iteration number is also that of the computational time.

Case 1: Lid-Driven Flow in a Square Cavity

Computations are conducted at $\text{Re} = 1,000$, which is defined as

$$\text{Re} = \frac{U_{\text{Lid}} L}{\nu} \tag{38}$$

Here U_{Lid} is the moving velocity of the upper lid, and L stands for the length of the cavity. In Figure 4, the numerical results with the new algorithm are compared with the benchmark solution provided by Ghie et al. [20], where X and Y are nondimensional coordinates, normalized by the cavity length L, and U, V are the nondimensional velocities, normalized by the U_{Lid}. We can see that the present results of velocity distributions along the centerlines agree well with the benchmark solutions, which proves the accuracy of the CLEARER algorithm.

The iteration numbers of the SIMPLER and CLEARER algorithms are compared in Figure 5. It can be seen that the iteration number required by the CLEARER algorithm is always lower than that required by the SIMPLER algorithm. Both algorithms can get the convergent solution in a large range of underrelaxation factors, and it also shows that the robustness of CLEARER is no lower than that of SIMPLER. The ratio of iteration number of CLEARER over SIMPLER is seen in Figure 6; we can see that in the region of high-value underrelaxation factor α, the CLEARER algorithm has better convergence performance than SIMPLER. In the range of variation of α, the ratio of iteration number ranges from 0.25 to 0.73.

Case 2: Natural Convection in a Square Cavity

Natural convection is studied in a square cavity, with top and bottom walls adiabatic while the left and right walls are kept at a constant but different temperature. The average Nusselt number Nu near the wall and the maximum velocities at the centerlines at $\text{Ra} = 10^5$ are compared with the benchmark solutions [21], as shown in Table 2, from which we can see that the agreement is quite satisfactory.

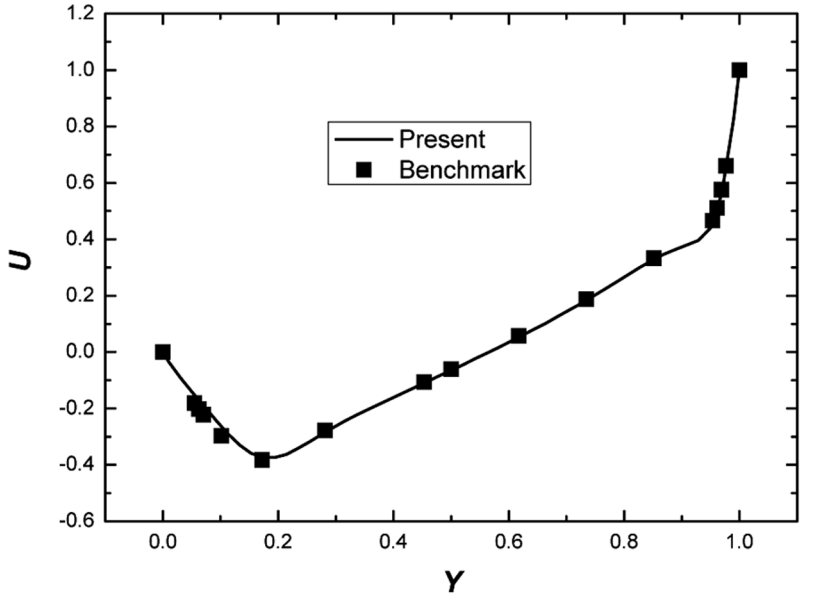

(*a*) U velocity distribution along $X = 0.5$

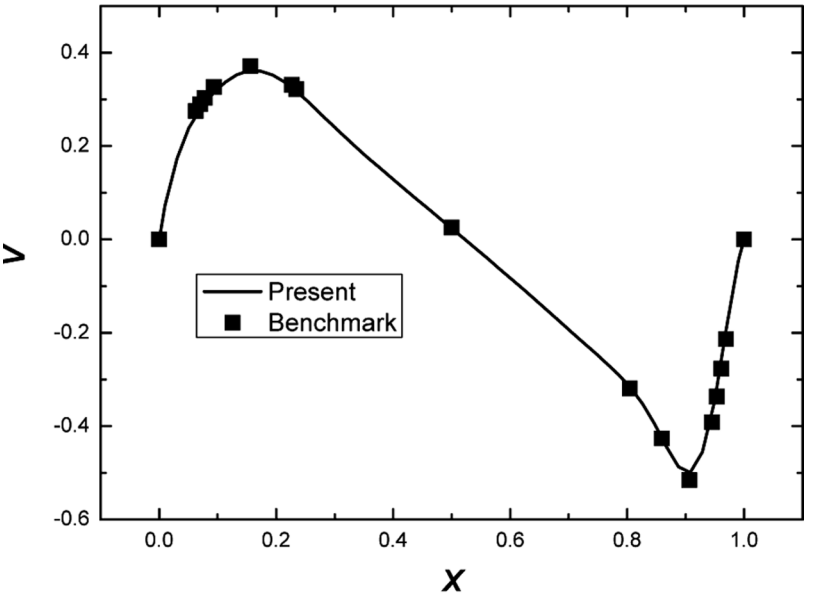

(*b*) V velocity distribution along $Y = 0.5$

Figure 4. Comparison between predicted velocity distributions and benchmark solution.

From Figure 7 we can see that both the CLEARER and SIMPLER algorithms are quite robust in that the underrelaxation factor α can vary from 0.1 to 0.99, while the CLEARER algorithm always needs fewer iterations than the

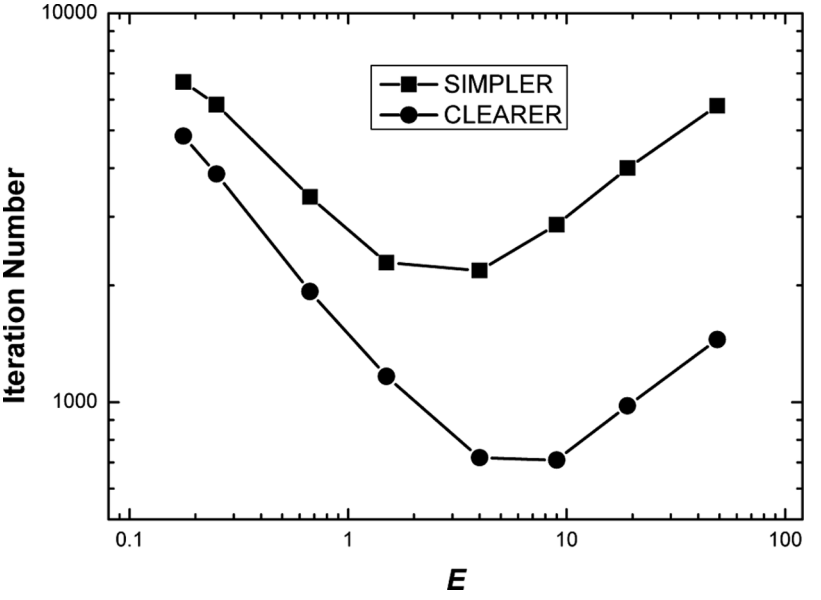

Figure 5. Comparison of iteration number between SIMPLER and CLEARER.

SIMPLER algorithm to reach the same convergence criterion. The ratio of iteration number of CLEARER over SIMPLER ranges from 0.47 to 0.88, which is shown in Figure 8.

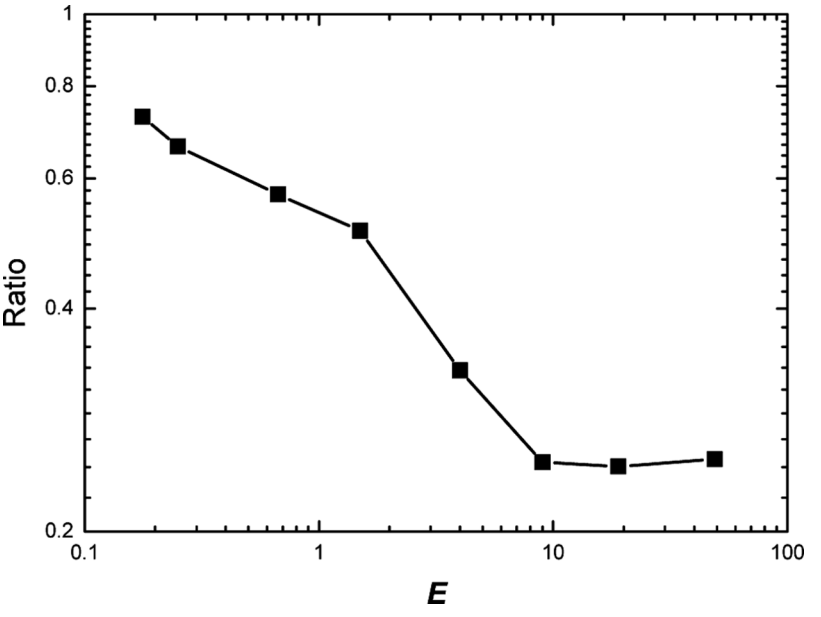

Figure 6. Ratio of iteration number of CLEARER versus SIMPLER.

Table 2. Comparison of predicted results with benchmark solutions at $Ra = 10^5$

	Nu_m	U_{max}	Y_{max}	V_{max}	X_{max}
Benchmark	4.510	0.132	0.859	0.258	0.066
Present	4.584	0.131	0.847	0.256	0.071

Case 3: Lid-Driven Flow in a Polar Cavity

The configuration of the polar cavity is shown in Figure 9; here $\theta = 1$ rad and $\delta/R_{in} = 1$. The Reynolds number is defined as

$$Re = \frac{U_{Lid}\delta}{\nu} \tag{39}$$

where $U_{Lid} = R_{in}\omega$ is the circumferential velocity of the moving lid. The streamlines in the polar cavity at $Re = 1{,}000$ are compared with the results provided by Fuchs and Tillmark [22], as seen in Figure 10, from which we can see that they agree quite well.

The iteration numbers of the CLEARER and SIMPLER algorithms are compared in Figure 11. It is found that when the underrelaxation factor $\alpha = 0.98$, a convergent solution cannot be obtained with the SIMPLER algorithm, while with the CLEARER algorithm we can still get a convergent solution, which indicates that CLEARER is more robust than SIMPLER. From Figure 12 we can see that the ratio of iteration number of CLEARER over SIMPLER ranges from 0.21 to 0.58, which proves the excellent convergence characteristic of the CLEARER algorithm.

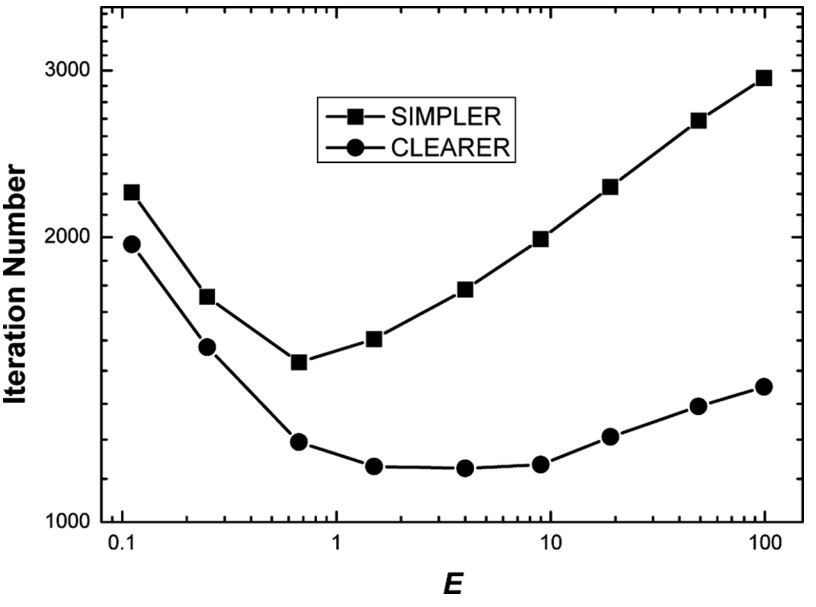

Figure 7. Comparison of iteration number between SIMPLER and CLEARER.

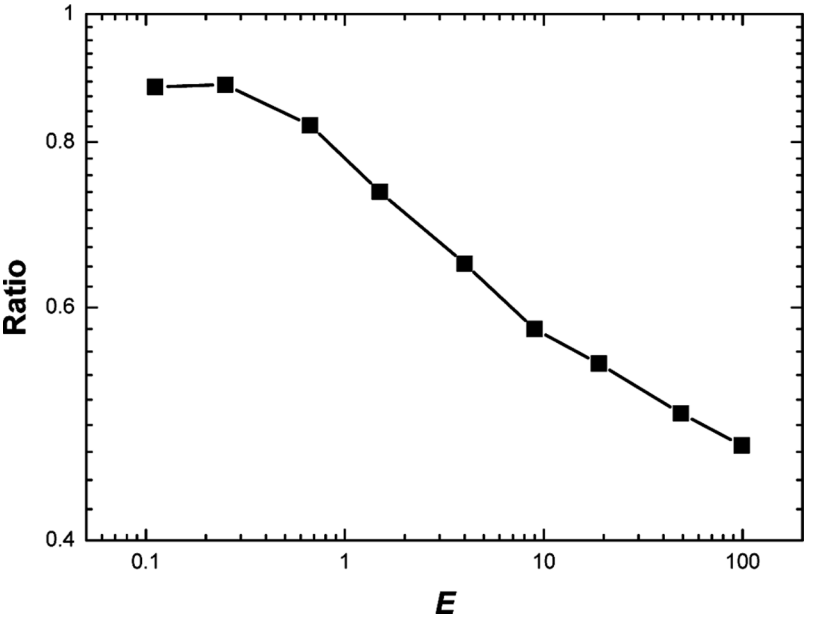

Figure 8. Ratio of iteration number of CLEARER versus SIMPLER.

Case 4. Natural Convection in an Annular Enclosure

The natural convection between two horizontal concentric cylinders is depicted in Figure 13, where the inner cylinder is kept at high temperature and the outer cylinder is at low temperature. $\mathrm{Ra} = 5 \times 10^4$ and is defined as

$$\mathrm{Ra} = \frac{\rho g \beta \delta^3 \delta T}{a \eta} \tag{40}$$

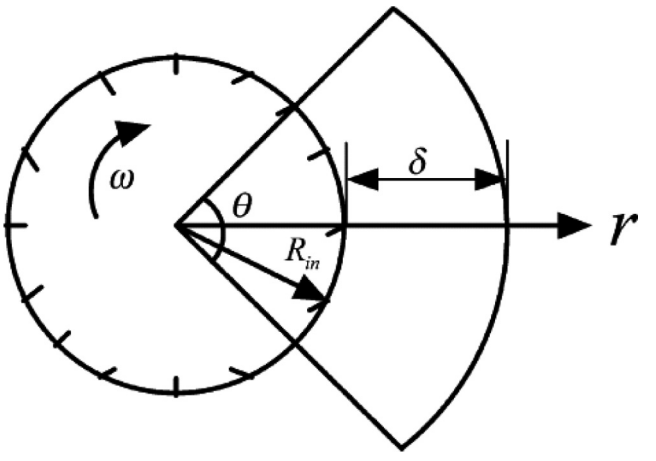

Figure 9. Lid-driven flow in a polar cavity.

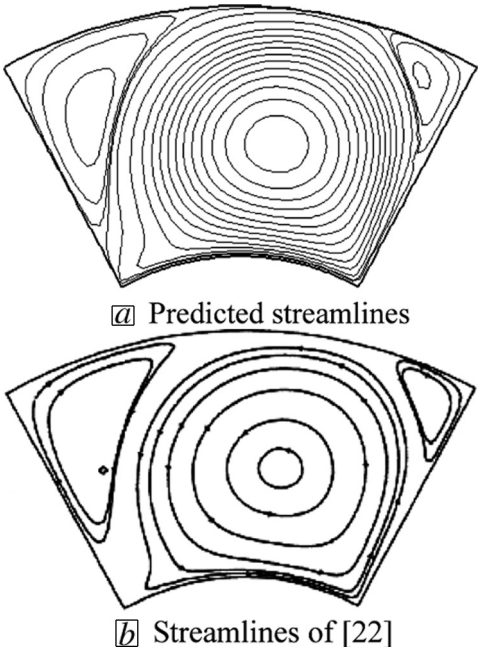

Figure 10. Comparison of streamlines at Re = 1,000.

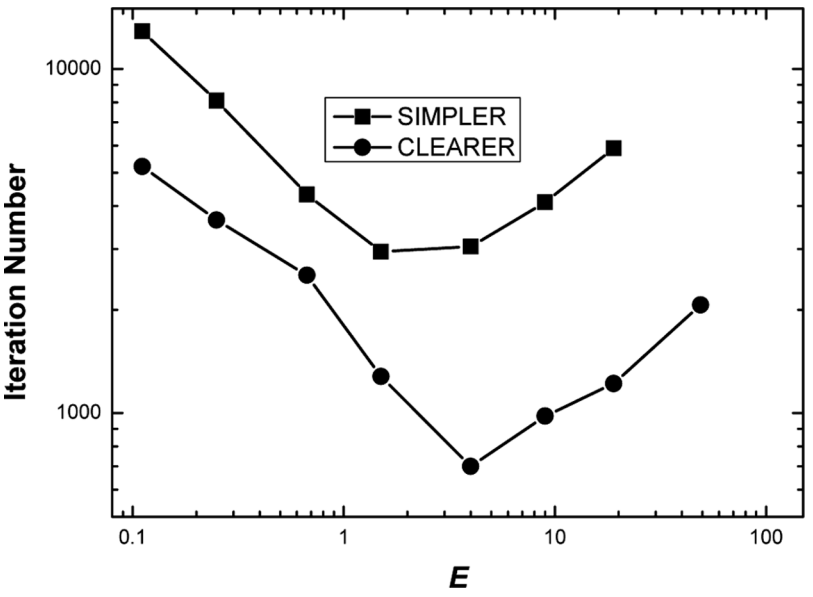

Figure 11. Comparison of iteration number between SIMPLER and CLEARER.

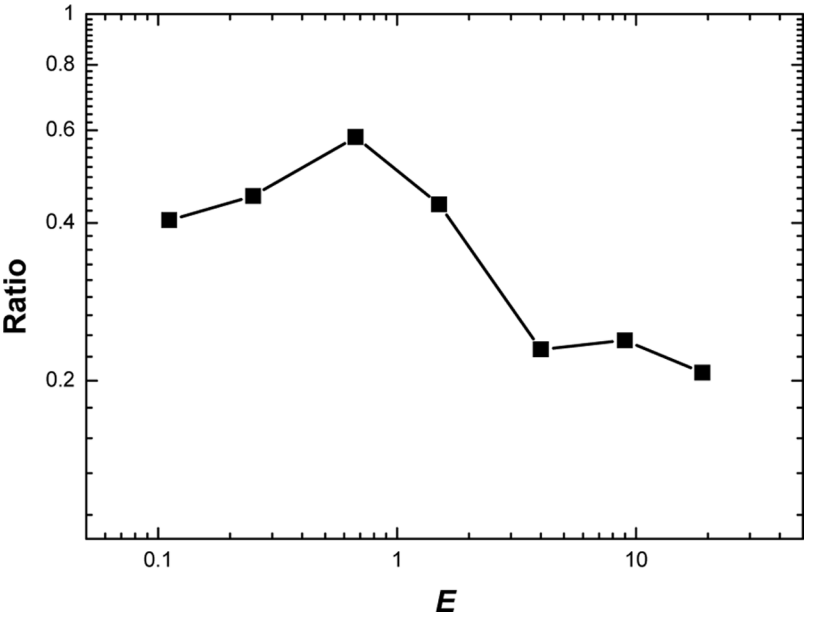

Figure 12. Ratio of iteration number of CLEARER versus SIMPLER.

Kuehn and Goldstein [23] have studied this case through both numerical simulation and experiment. In Figure 14 the streamlines and isothermals are compared with their results, which show good agreement.

For accurate comparison, the heat transfer performance around the inner and outer cylinders is compared with the results of Kuehn and Goldstein [23]. For the

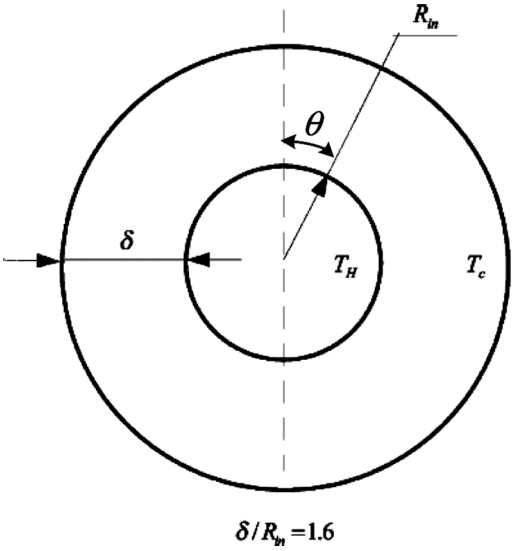

Figure 13. Natural convection in a concentric cylinder.

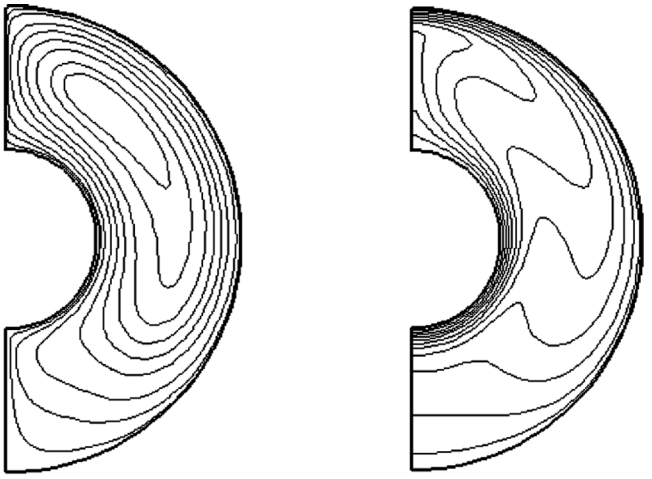

(*a*) Streamlines (*b*) Isothermals

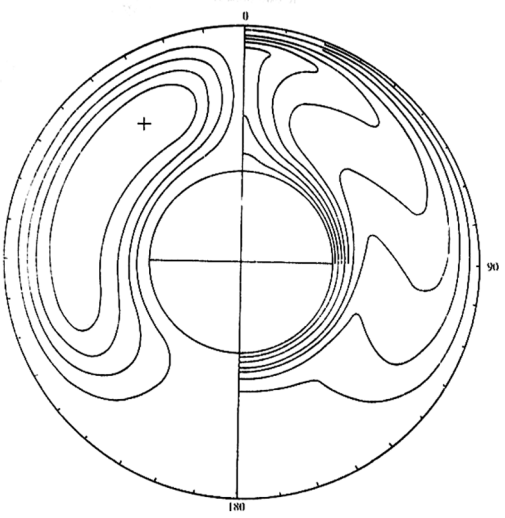

(*c*) Streamlines and isothermals of [23]

Figure 14. Comparison of streamlines and isothermals at $\mathrm{Ra} = 5 \times 10^4$.

natural convection between two concentric cylinders, the local equivalent conductivity is often used to evaluate the heat transfer performance, which is defined as follows.

For the inner cylinder:

$$K_{\mathrm{eq}} = -R_{\mathrm{in}} \ln\left(\frac{R_{\mathrm{in}} + \delta}{R_{\mathrm{in}}}\right) \frac{\partial T}{\partial R} \tag{41a}$$

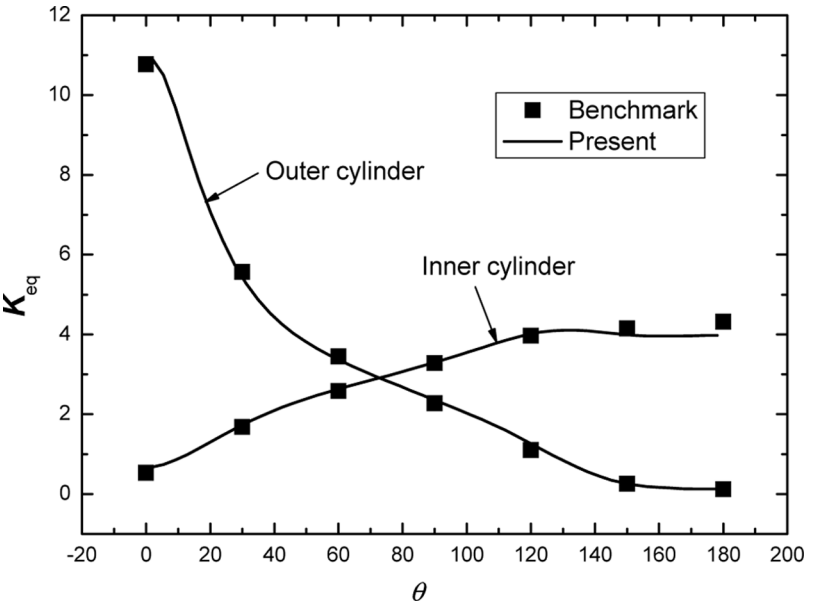

Figure 15. Comparison of distribution of local equivalent conductivity.

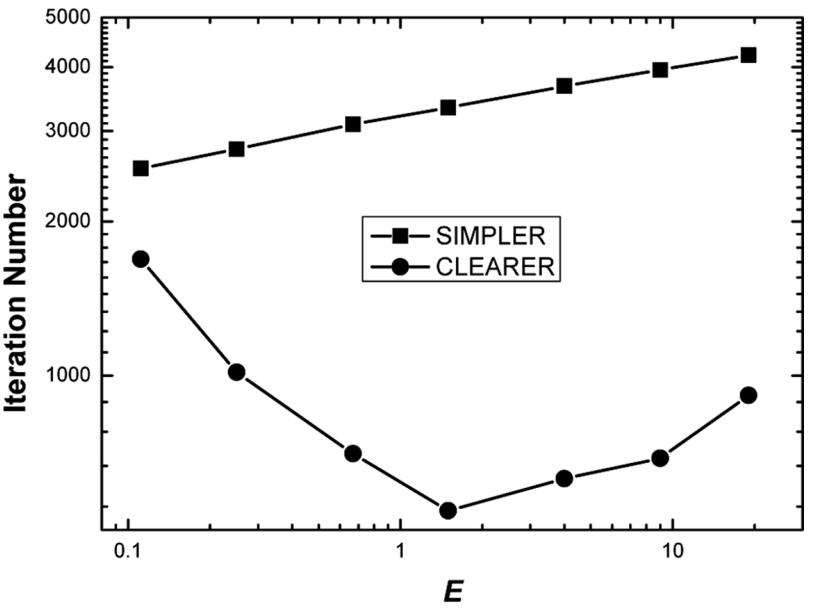

Figure 16. Comparison of iteration number between SIMPLER and CLEARER.

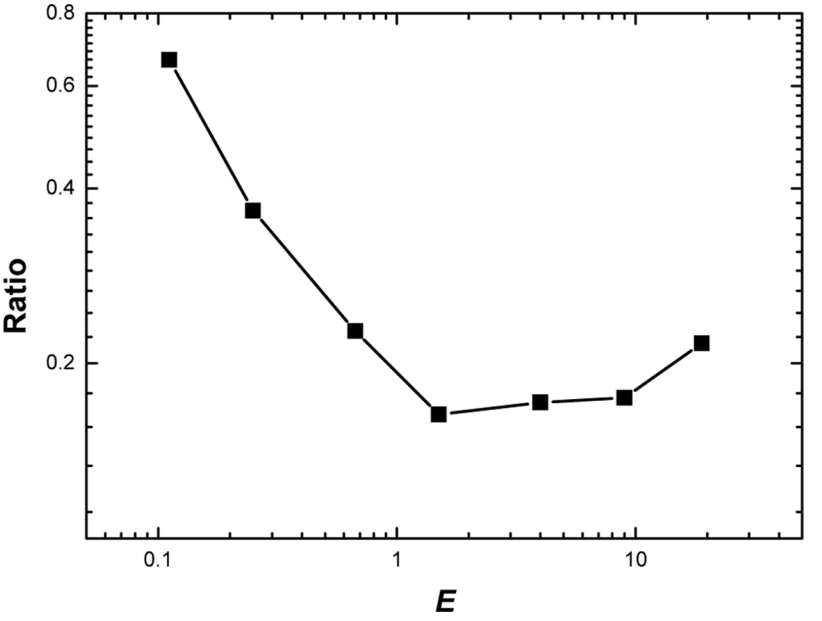

Figure 17. Ratio of iteration number of CLEARER versus SIMPLER.

For the outer cylinder:

$$K_{eq} = -(R_{in} + \delta) \ln\left(\frac{R_{in} + \delta}{R_{in}}\right) \frac{\partial T}{\partial R} \tag{41b}$$

From Figure 15 we can see that the distribution of local equivalent conductivity around both the inner cylinder and the outer cylinder agrees well with the benchmark solutions.

The iteration numbers for SIMPLER and CLEARER are compared in Figure 16, from which we can see that the CLEARER algorithm always has a much lower iteration number than the SIMPLER algorithm, especially when the underrelaxation α is quite large. Furthermore, the robustness of CLEARER is no lower than that of SIMPLER. Figure 17 shows that the ratio of iteration number for CLEARER over SIMPLER ranges from 0.17 to 0.67.

CONCLUSION

In this article, the CLEARER algorithm on a collocated grid has been proposed based on the idea of the CLEAR algorithm. Then four numerical examples with reliable solutions have been calculated to validate the algorithm, and the performance of the CLEARER and SIMPLER algorithms has been compared. The major conclusions are summarized as follows.

1. In the SIMPLER algorithm on a collocated grid, the velocities on the main nodes are overcorrected by the pressure correction.

2. A second relaxation factor is introduced in calculating the interface velocities in the corrector step, and the convergent solution is independent of this factor. By keeping the second relaxation factor smaller than the underrelaxation factor for velocity, the convergence rate can be speeded up greatly.
3. Numerical results with the CLEARER algorithm agree well with the benchmark solutions.
4. The CLEARER algorithm has higher robustness and better convergence performance than the SIMPLER algorithm, and in some cases the ratio of the iteration number of CLEARER over SIMPLER can be as low as 17%.

REFERENCES

1. S. V. Patankar and D. B. Spalding, A Calculation Procedure for Heat, Mass and Momentum Transfer in Three-Dimensional Parabolic Flows, *Int. J. Heat Mass Transfer*, vol. 15, pp. 1787–1806, 1972.
2. C. M. Rhie and W. L. Chow, Numerical Study of the Turbulent Flow Past an Airfoil with Trailing Edge Separations, *AIAA J.*, vol. 21, pp. 1525–1535, 1983.
3. M. C. Melaaen, Calculation of Fluid Flows with Staggered and Non-staggered Curvilinear Non-orthogonal Grids—A Comparison, *Numer. Heat Transfer B*, vol. 21, pp. 21–39, 1992.
4. S. K. Choi, N. H. Yun, and M. Cho, Use of Staggered and Nonstaggered Grid Arrangements for Incompressible Flow Calculations on Nonorthogonal Grids, *Numer. Heat Transfer B*, vol. 25, pp. 193–204, 1994.
5. S. K. Choi, N. H. Yun, and M. Cho, Systematic Comparison of Finite Volume Methods with Staggered and Nonstaggered Grid Arrangements, *Numer. Heat Transfer B*, vol. 25, pp. 205–221, 1994.
6. S. Majumdar, Role of Underrelaxation in Momentum Interpolation for Calculation of Flow with Nonstaggered Grids, *Numer. Heat Transfer*, vol. 13, pp. 125–132, 1988.
7. T. F. Miller and F. W. Schmidt, Use of a Pressure-Weighted Interpolation Method for the Solution of Incompressible Navier-Stokes Equations on a Non-staggered Grid System, *Numer. Heat Transfer*, vol. 14, pp. 213–233, 1988.
8. M. H. Kobayashi and J. C. F. Perira, Numerical Comparison of Momentum Interpolation Methods and Pressure-Velocity Algorithm Using Nonstaggered Grids, *Commum. Appl. Numer. Mech.*, vol. 7, pp. 173–196, 1991.
9. S. K. Choi, Note on the Use of Momentum Interpolation Method for Unsteady Flows, *Numer. Heat Transfer A*, vol. 36, pp. 545–550, 1999.
10. B. Yu, Y. Kawaguchi, W. Q. Tao, and H. Ozoe, Checkerboard Pressure Predictions due to the Underrelaxation Factor and Time Step Size for a Nonstaggered Grid with Momentum Interpolation Method, *Numer. Heat Transfer B*, vol. 41, pp. 85–94, 2002.
11. B. Yu, W. Q. Tao, J. J. Wei, Y. Kawaguchi, T. Tagawa, and H. Ozoe, Discussion on Momentum Interpolation Method for Collocated Grids of Incompressible Flow, *Numer. Heat Transfer B*, vol. 42, pp. 141–166, 2002.
12. W. Q. Tao, Z. G. Qu, and Y. L. He, A Novel Segregated Algorithm for Incompressible Fluid Flow and Heat Transfer Problems—CLEAR (Coupled and Linked Equations Algorithm Revised) Part I: Mathematical Formulation and Solution Procedure, *Numer. Heat Transfer B*, vol. 45, pp. 1–17, 2004.
13. W. Q. Tao, Z. G. Qu, and Y. L. He, A Novel Segregated Algorithm for Incompressible Fluid Flow and Heat Transfer Problems—CLEAR (Coupled and Linked Equations Algorithm Revised) Part II: Application Examples, *Numer. Heat Transfer B*, vol. 45, pp. 19–48, 2004.

14. Z. G. Qu, W. Q. Tao, and Y. L. He, Implementation of CLEAR Algorithm on Collocated Grid System and Application Examples, *Numer. Heat Transfer B*, vol. 46, pp. 65–96, 2005.
15. W. Q. Tao, *Numerical Heat Transfer*, 2nd ed., Xi'an Jiaotong University Press, Xi'an, China, 2001.
16. S. V. Patankar, *Numerical Heat Transfer and Fluid Flow*, Hemisphere, Washington, DC, 1980.
17. Z. Y. Li and W. Q. Tao, A New Stability-Guaranteed Second-Oder Difference Scheme, *Numer. Heat Transfer B*, vol. 42, pp. 349–365, 2002.
18. W. F. Ames, *Numerical Methods for Partial Differential Equations*, 2nd ed., Academic Press, New York, 1977.
19. C. Prakash and S. V. Patankar, Combined Free and Forced Convection in Vertical Tube with Radial Internal Fin, *ASME J. Heat Transfer*, vol. 7, pp. 566–572, 1981.
20. U. Ghie, K. N. Ghie, and C. T. Shin, High-Re Solution for Incompressible Flow Using the Navier-Stokes Equations and a Multigrid Method, *J. Comput. Phys.*, vol. 48, pp. 387–411, 1982.
21. G. Barakos and E. Mitsoulis, Natural Convection Flow in a Square Cavity Revisited: Laminar and Turbulent Models with Wall Function, *Int. J. Numer. Meth. Fluids*, vol. 18, pp. 695–719, 1994.
22. L. Fuchs and N. Tillmark, Numerical and Experimental Study of Driven Flow in a Polar Cavity, *Int. J. Numer. Meth. Fluids*, vol. 5, pp. 311–329, 1985.
23. T. H. Kuehn and R. J. Goldstein, An Experimental and Theoretical Study of Natural Convection in the Annulus between Horizontal Concentric Cylinders, *J. Fluid Mech.*, vol. 74, pp. 695–715, 1969.